



Published in final edited form as:

Ann Neurol. 2023 August ; 94(2): 232–244. doi:10.1002/ana.26676.

The associations of VGF with neuropathologies and cognitive health in older adults

Lei Yu, PhD^{1,2}, Vladislav A. Petyuk, PhD³, Katia de Paiva Lopes, PhD^{1,2}, Shinya Tasaki, PhD^{1,2}, Vilas Menon, PhD⁴, Yanling Wang, PhD^{1,2}, Julie A. Schneider, MD^{1,2,5}, Philip L. De Jager, MD, PhD⁴, David A. Bennett, MD^{1,2}

¹ Rush Alzheimer's Disease Center, Rush University Medical Center; Chicago, IL, USA.

² Department of Neurological Sciences, Rush University Medical Center; Chicago, IL, USA.

³ Pacific Northwest National Laboratory; Richland, WA, USA.

⁴ Center for Translational and Computational Neuroimmunology, Department of Neurology & Taub Institute for Research on Alzheimer's disease and the Aging Brain, Columbia University Irving Medical Center; New York, NY, USA.

⁵ Department of Pathology, Rush University Medical Center; Chicago, IL, USA.

Abstract

Objective: VGF is proposed as a potential therapeutic target for Alzheimer's (AD) and other neurodegenerative conditions. The cell-type specific and, separately, peptide specific associations of VGF with pathologic and cognitive outcomes remain largely unknown. We leveraged gene expression and protein data from the human neocortex and investigated the VGF associations with common neuropathologies and late-life cognitive decline.

Methods: Community-dwelling older adults were followed every year, died and underwent brain autopsy. Cognitive decline was captured via annual cognitive testing. Common neurodegenerative and cerebrovascular conditions were assessed during neuropathologic evaluations. Bulk brain RNASeq and targeted proteomics analyses were conducted using frozen tissues from dorsolateral prefrontal cortex of 1,020 individuals. Cell-type specific gene expressions were quantified in a subsample (N=424) following single nuclei RNASeq analysis from the same cortex.

Results: The bulk brain *VGF* gene expression was primarily associated with AD and Lewy bodies. The *VGF* gene association with cognitive decline was in part accounted for by neuropathologies. Similar associations were observed for the VGF protein. Cell-type specific analyses revealed that, while *VGF* was differentially expressed in most major cell types in the cortex, its association with neuropathologies and cognitive decline was restricted to the neuronal

Corresponding Author: Lei Yu, Rush Alzheimer's Disease Center, 1750 W Harrison Street, Suite 1000, Chicago, IL 60612, Lei_Yu@rush.edu.

Authors Contributions

LY, VAP and DAB contributed to the conception and design of the study; LY, VAP, KdPL, ST, VM and JAS contributed to the acquisition and analysis of data; All authors contributed to drafting the text.

Potential Conflicts of Interest

Nothing to report.

cells. Further, the peptide fragments across the VGF polypeptide resemble each other in relation to neuropathologies and cognitive decline.

Interpretation: Multiple pathways link VGF to cognitive health in older age, including neurodegeneration. The *VGF* gene functions primarily in neuronal cells and its protein associations with pathologic and cognitive outcomes do not map to a specific peptide.

Introduction

Alzheimer's disease (AD) and other neurodegenerative conditions are the key drivers of cognitive impairment and dementia in older age. Identifying therapeutic targets that protect against the detrimental effects of these brain pathologies is pivotal for healthy cognitive aging. Neurodegeneration leads to loss of synapses and neurons, and subsequently cognitive deficits¹⁻³. Neurotrophins are a family of secretory proteins that regulate neural activity and synaptic plasticity⁴. VGF (non-acronymic), which is induced by neurotrophins, encodes a 68 kDa protein precursor that is cleaved into multiple smaller biologically active neuroendocrine peptides^{5, 6}. VGF expression is lower in neurodegenerative disorders including AD, amyotrophic lateral sclerosis (ALS), and Parkinson's disease (PD)⁷⁻¹⁰. In cerebrospinal fluid (CSF), VGF is correlated with amyloid and phosphorylated tau, the pathologic hallmarks of AD¹¹. Multiscale causal networks analysis further identifies VGF as a regulator of AD¹². Dysregulated VGF is also implicated in cognition. A proteome-wide association study finds that a lower VGF level in human cortex was associated with cognitive decline, with or without adjusting for AD pathology¹³. Together, these data highlight the role of VGF as a potential biomarker and therapeutic target for neurodegeneration¹⁴.

For better understanding of the relationships between VGF, neuropathologies and downstream cognitive outcomes, further investigations are warranted in the following areas. First, the extent to which VGF is implicated in non-AD degenerative and cerebrovascular pathologies has not been systematically examined. As mixed pathologies account for a majority of dementia cases^{15, 16}, it is important to disentangle the associations of VGF with the complex constellations of neuropathologies that commonly coexist in the aging brain. Second, data for cellular *VGF* expressions in human cortex is just starting to emerge, and cell-type specific associations of *VGF* with neuropathologies and cognitive outcomes remain poorly understood. Third, VGF is proteolytically processed into at least 12 peptides, and each has diverse biological functions^{5, 14}. Identifying specific bioactive peptides that protect against neurodegeneration would greatly facilitate target nomination. Current experiments largely focus on the C-terminal peptide of TLQP-62 given its role in BDNF-TrkB signaling activation^{12, 17, 18}, but other peptides (e.g. AQEE-30 and TLQP-21) are also implicated in synaptic plasticity and microglial β amyloid clearance¹⁹⁻²¹. Whether the VGF involvement in neuropathologies and cognition is peptide-specific is unknown.

To fill these knowledge gaps, we interrogated VGF gene expression and protein data with neuropathologies and cognitive outcomes from over 1,000 community dwelling older adults who had participated in one of the two cohort studies of aging, died and undergone brain autopsies. Specifically, *VGF* gene expression values were obtained from bulk RNASeq,

separately from single-nuclei RNASeq (snRNASeq), and the abundance of 11 VGF peptide fragments were measured using selected reaction monitoring (SRM) proteomics. All these data were collected using frozen tissues of dorsolateral prefrontal cortex (DLPFC). For each layer of the VGF data, we examined its association with a host of neuropathologic indices (i.e., AD, Lewy bodies, hippocampal sclerosis, limbic-predominant age-related TDP-43 encephalopathy (LATE), cerebrovascular infarcts, and vessel diseases), as well as late-life cognitive decline.

Methods

Study cohorts

Data was obtained from deceased participants in the Religious Orders Study (ROS) or Rush Memory and Aging Project (MAP). ROS and MAP are two clinical neuropathologic cohort studies of aging that focus on Alzheimer's disease and related dementias²². Participants were enrolled without known dementia, all agreed to annual home visits and brain donation at death. Each study was approved by an institutional review board of Rush University Medical Center, and was conducted according to the Declaration of Helsinki. At enrollment, a written informed consent and an Anatomical Gift Act were received from each participant.

By late October 2022, 2,250 ROSMAP participants had died, over 85% had undergone brain autopsies (N=1,933), and 1,879 individuals had neuropathologic evaluations approved by a board-certified neuropathologist. RNASeq and proteomics data collection are ongoing. At the time of these analyses, Bulk RNASeq and SRM proteomics data were collected from 1,020 individuals, and snRNASeq data was available in a subsample of 424 individuals.

Cognitive assessments

At annual home visits, participants were administered an approximately 1-hour long cognitive assessment that includes 21 tests, 19 of which assess performance in multiple cognitive domains of episodic memory, semantic memory, working memory, perceptual speed and visuospatial ability. At each visit, raw scores for each test were standardized using the baseline mean and standard deviation (SD) of the entire cohorts, and then standardized scores were averaged across the 19 tests to obtain a composite measure for global cognition. This repeated measure of annual global cognitive scores allows us to trace individual cognitive trajectories from baseline until death and was used for estimating longitudinal cognitive decline.

Neuropathologic evaluations

After a participant died, study coordinators worked with the designated contact and funeral home to arrange for brain autopsy²³. The postmortem interval had a mean of 8.3 hours (SD: 6.0). Brain was removed, weighed and one hemisphere immediately cut coronally into 1cm slabs. One hemisphere was frozen in a -80 °C freezer for biochemical studies, and the other was fixed in 4% paraformaldehyde for neuropathologic evaluations.

Neuropathologic evaluations of AD, non-AD degeneration, and cerebrovascular conditions were conducted following a standard and uniform protocol. AD diagnosis was based on

the modified NIA-Reagan criteria²⁴. Data for β -amyloid load and paired helical filaments (PHF) tau tangles density were also collected by immunohistochemistry²⁵. Sections (6 μ m) from midfrontal, midtemporal and inferior parietal were immunostained using α -synuclein antibodies for detecting neocortical Lewy bodies²⁶. Hippocampal sclerosis was determined using haematoxylin and eosin (H&E) stained sections from midhippocampus²⁷. LATE neuropathologic changes (LATE-NC) was assessed by immunohistochemistry using antibodies to phosphorylated TDP43. Based on the progression of TDP43 cytoplasmic inclusions across varying brain regions, a 4-stage LATE-NC measure was obtained as 0: no inclusion, 1: inclusion localized to amygdala, 2: inclusion extended to hippocampus and entorhinal cortex, and 3: inclusion extended to neocortex²⁸.

Chronic macroscopic infarcts were identified during gross examination and confirmed histologically. Chronic microinfarcts were detected using H&E stained sections from at least 9 regions²⁹. Amyloid deposition in the vessels (CAA) was assessed using immunostained sections from midfrontal, midtemporal, parietal, and calcarine cortices³⁰. Arteries and their proximal branches in the circle of Willis were visually examined for atherosclerosis, and H&E stained sections from basal ganglia was inspected for arteriolosclerosis³¹. CAA, atherosclerosis and arteriolosclerosis were graded on a semiquantitative scale of none, mild, moderate or severe.

Bulk and single nuclei RNASeq

The bulk RNASeq analysis was conducted on frozen tissues from DLPFC, as previously described³². Briefly, RNA sequencing was performed in three batches. For each batch, the process involves samples extraction, RNA quality and quantity check, and sequencing library construction. Paired ended sequences were aligned to a human reference genome and annotated. Picard tools were used for data quality check. Raw counts for individual transcripts were quantified and aggregated for each gene. For downstream normalization, we included approximate 17,500 genes that were expressed in over half of the samples with at least 10 counts in each sample. The gene counts were adjusted for guanine-cytosine (GC) content and gene length using conditional quantile normalization, and then converted to counts per million. After log₂ transform, a linear regression model was performed to regress out key technical confounders including sequencing batch, RNA quality, and total spliced reads³³.

The snRNASeq analysis was also conducted on frozen tissues from DLPFC³⁴. Nuclei were isolated from each donor, and then pooled together (8 donors per batch) for library preparation. Library construction was performed using the 10x Genomics Chromium platform with 3'-version 3 chemistry. Cell Ranger was used for read alignment and to generate unique molecular identifier counts³⁵. The pooled samples within batch were demultiplexed by comparing the genetic information in RNA reads with the whole genome sequencing data from the same individuals. Data were checked for genotype discordance, sex discordance, duplicates, and sequencing depth. As a result, 424 out of the initial 479 samples (89%) passed quality controls.

Nuclei were annotated into 7 major cell types, i.e., astrocytes, endothelial cells, excitatory neurons, inhibitory neurons, microglia, oligodendrocyte precursor cells (OPC), and

oligodendrocytes. Doublets were removed using DoubletFinder³⁶ and nuclei were clustered using Seurat³⁷. Pseudo-bulk matrices were generated by summing counts per major cell type per sample. Within each cell type, we retained genes with counts per million > 1 in 80% of samples. Finally, the TMM-voom method for normalization was applied to the individual count matrices³⁸. For statistical analyses, data for bulk and cell type specific *VGF* gene expressions were extracted from the final processed RNASeq data matrices.

SRM proteomics of VGF

The VGF protein data came from the same DLPPFC tissue. Details on SRM proteomics analysis for ROSMAP samples were previously reported³⁹. Briefly, Brain tissues were homogenized, denatured, and subject to tryptic digestion. After C18 SPE cleaning and concentration adjustment, the tryptic digests were mixed with synthetic peptide mix. A total of 19 VGF tryptic peptides were designed for targeted analysis (Supplementary Table 1). We were able to confidently quantify 11 after testing for sensitivity and quality of quantification. Importantly, these 11 VGF peptide fragments were spread across the entire sequence of the VGF precursor (Figure 1). Some of these peptide fragments represent surrogates of known bioactive VGF peptides (e.g. NERPs and TLQPs), and some match the VGF peptides detected in human CSF that were implicated in AD (e.g. NSEP-17 or VGF_{64–80})⁴⁰.

The SRM experiments were performed on an ACQUITY UPLC coupled to TSQ Vantage mass spectrometry instrument, with 1 µg sample injection for each measurement. The data were analyzed by Skyline⁴¹. All peak assignment and boundaries were manually checked. The peak area ratios of endogenous light peptides to their heavy isotope-labeled internal standards were calculated and the transitions without matrix interference were used for accurate quantification. The relative abundances for individual peptides were log₂ transformed and centered at the median.

Statistical analyses

For each neuropathologic index separately, we examined the VGF associations using logistic or linear regression as appropriate (Supplementary Methods). In these models, individual pathologic index was the outcome and the bulk *VGF* gene expression or protein abundance was the predictor. To reduce false positives, we applied the Bonferroni correction to adjust the Type-1 error for the 11 neuropathologic indices tested, i.e., $\alpha_{adj}=0.05/11\sim 0.005$. Late life cognitive decline was estimated by fitting linear mixed effects models to the longitudinal data of annual cognitive scores. A key term of the model was time in years before death, which estimates the mean slope of change in cognition. The core model included the terms for age, sex and education, as well as their interactions with time. Next, we added a term for the *VGF* gene expression and its interaction with time. The interaction estimates the association of *VGF* with cognitive decline. To further adjust for neuropathologies, we repeated the model by including additional terms for 10 neuropathologic indices, i.e., β -amyloid load, PHFtau tangles density, neocortical Lewy bodies, hippocampal sclerosis, LATE-NC, macroscopic infarcts, microinfarcts, CAA, atherosclerosis and arteriolosclerosis, and their interactions with time. The proportion of reduction in the *VGF* by time interaction between the two models estimates the extent to which the *VGF* association with cognitive

decline is due to neuropathologies. Similar analyses were conducted for cell type specific *VGF* gene expression and VGF protein.

Results

Characteristics of study participants

On average, participants enrolled at age of 81 (SD: 6.9) and died at 89 (SD: 6.5). A majority were females. At death, 33% were cognitively unimpaired, 24% were mild cognitively impaired and the remaining 43% had dementia. There was a significant decline in cognition over a mean of 8 annual follow-ups, such that the mean cognitive score dropped by approximately 1SD every decade (Estimate for annual rate of change: -0.11 , Standard error [SE]: 0.004, $p < 0.001$).

Over 60% of the individuals met pathologic criteria for AD. Approximately 12% had Lewy bodies in neocortex, 10% had hippocampal sclerosis (defined as severe neuronal loss and gliosis in hippocampus), 31% had TDP43 pathology extended beyond amygdala, and more than half had LATE-NC Stage 1 or greater, with or without hippocampal sclerosis. Separately, half of the individuals had macroscopic or microinfarcts and two thirds had moderate or severe CAA, atherosclerosis, or arteriolosclerosis (Table 1).

Cortical *VGF* gene expression is associated with neuropathologies and cognitive decline

We first examined the associations of bulk *VGF* gene expression in DLPFC with individual neuropathologic indices. The associations were primarily restricted to neurodegenerative pathologies (Figure 2A). Specifically, higher *VGF* expression was associated with lower odds of pathologic AD. Similar results were observed for the continuous measures of β amyloid load (B: -0.207 , SE: 0.036, $p < 0.001$) and tangles density (B: -0.235 , SE: 0.038, $p < 0.001$). In addition, higher *VGF* expression was also associated with lower odds of neocortical Lewy bodies and LATE-NC. The *VGF* association with neocortical Lewy bodies was unchanged after controlling for AD pathologies. By contrast, the association with LATE-NC was attenuated and no longer significant. Our data did not show a *VGF* association with hippocampal sclerosis, infarcts, CAA or arteriolosclerosis, but surprisingly higher *VGF* was associated with more severe atherosclerosis.

Consistent with the results for neuropathologies, higher *VGF* expression was associated with slower cognitive decline (Figure 3A). This result persisted after adjusting for the neuropathologies (Figure 3B). However, attenuation of the *VGF* association was noticeable. Before adjustment, with 1SD greater *VGF* expression, the slope of cognitive decline was 0.018 standard unit slower (SE: 0.003, $p < 0.001$). After adjustment, the estimate was reduced to 0.008 (SE: 0.003, $p = 0.008$), suggesting that over half of the association was likely mediated by neuropathologies.

Cortical *VGF* gene expression association is driven by neuronal cell types

By leveraging the snRNASeq data from 424 individuals, we examined cellular *VGF* gene expressions and their associations with neuropathologies and cognitive decline. Of note, the demographic and clinicopathologic characteristics for this subsample were similar to

the overall study participants (Table 1). *VGF* gene expressions were detected in 6 of the 7 major cell types except for endothelial cells (Figure 4A). The expression level is highest in excitatory neurons and lowest in astrocytes. A mixed effects analysis of variance suggests that *VGF* was differentially expressed across these 6 cell types ($F_{5,2115} = 234.7$, $p < 0.001$). The *VGF* expressions in the two major neuronal cell types (glutamatergic/excitatory and GABAergic/inhibitory neurons) were highly correlated and high correlations were also observed between astrocytes, microglia and oligodendrocytes (Figure 4B).

Interestingly, cellular *VGF* gene expression associations with neuropathologies were detected only in excitatory and inhibitory neurons (Figure 4C). Similar to the bulk gene expression results, higher levels of neuronal *VGF* was associated with lower β -amyloid load and tangles density, as well as lower odds of pathologic AD and neocortical Lewy bodies. Further, we found an association with cognitive decline in both neuronal cell types. Each 1SD greater *VGF* expression in excitatory neurons was associated with 0.014 standard unit slower in the slope of cognitive decline (SE: 0.005, $p = 0.012$); for inhibitory neurons it was 0.021 standard unit (SE: 0.006, $p < 0.001$). No associations were found for other cell types. The *VGF* association in excitatory neurons did not survive the correction for multiple testing, but the result for inhibitory neurons persisted.

Cortical VGF protein is associated with neuropathologies and cognitive decline

The results of pairwise correlations for the 11 VGF peptide fragments showed that, with the exception of peptide #16 (Supplementary Table 1), all were moderately or highly correlated with one another (Figure 5A). A principal component analysis revealed that the first principal component (PC) explained over 65% of the total variance, and the eigenvalues for all the remaining PCs were all under 1 (Figure 5B). The abundances of individual peptides were averaged to obtain a composite measure for the protein abundance.

The protein composite was moderately correlated with the bulk *VGF* gene expression, with a Pearson r of 0.46. The results for the VGF protein composite with neuropathologies and cognitive decline were comparable with the bulk *VGF* gene expression. Specifically, the VGF protein level was inversely associated with AD, neocortical Lewy bodies, LATE-NC and CAA (Figure 2B). The association with neocortical Lewy bodies was independent of AD pathologies. The result for LATE-NC, and separately CAA, was attenuated and no longer significant after adjusting for AD. Higher VGF protein was associated with slower cognitive decline (Figure 3C and 3D). The estimates for the protein association with cognitive decline was 0.060 (SE: 0.006, $p < 0.001$) before and 0.021 (SE: 0.006, $p < 0.001$) after adjusting for the neuropathologies, suggesting that, similar to the result for the bulk *VGF* gene expression, over half of the protein association can be attributable to neuropathologies.

We further note that the bulk *VGF* gene expression was associated with cognitive decline through the VGF protein. With both bulk *VGF* gene expression and protein composite included in the same model, the association of *VGF* gene expression was attenuated from 0.018 (SE: 0.003, $p < 0.001$) to 0.004 (SE: 0.004, $p = 0.296$) and was no longer significant. In comparison, the VGF protein remained associated with cognitive decline with similar magnitude, where the estimate for the protein composite alone was 0.060 (SE: 0.006, p

<0.001) and 0.057 (SE: 0.007, $p < 0.001$) with *VGF* gene expression included in the same model.

Lack of peptide-specific VGF association with neuropathologies and cognitive decline

To test whether the association of VGF protein was driven by one or more specific peptides, we repeated the analyses by replacing the protein composite with the abundance of each of the 11 peptide fragments. Lack of peptide-specific association is evident. With the exception of peptide #16, multiple peptide fragments were associated with neurodegenerative indices of AD and neocortical Lewy bodies (Figure 5C). The results for cognitive decline were similar. Except for peptide #16, a 1-fold increase in the level of other VGF peptide corresponds to a slower rate of cognitive decline between 0.027 and 0.057 standard unit (Table 2). To contextualize, the average rate of cognitive decline for individuals with AD was -0.066 standard unit (SE=0.007, $p < .001$) faster than those without AD. So judging based on these estimates, the magnitude of association of these VGF peptides was between 40% and 85% of that of AD. Further, we note that peptide #16, with C-terminus corresponding to a product of an endogenous protease, is the sole partially-tryptic VGF peptide fragment quantified in our SRM analysis. This could explain why it acts differently in relation to neuropathologies as well as cognitive decline.

Discussion

In this work, we reported that cortical VGF are primarily related to neurodegenerative pathologies of AD and neocortical Lewy bodies, and approximately half of the VGF association with late life cognitive decline can be attributable to neuropathologies; the *VGF* gene expression level varies between major brain cell types, but the *VGF* association with neuropathologies and cognitive decline are restricted to neuronal cells; and finally almost all the VGF peptide fragments detected in the study show similar associations with neuropathologies and cognitive decline. These findings extend the current literature in several important ways.

We systematically interrogated the VGF associations with multiple degenerative and vascular indices in the brains of over 1,000 older adults. For both bulk RNA expression and protein abundance, higher cortical VGF level was associated with lower odds of AD, neocortical Lewy bodies and less severe LATE-NC. Of the three, the association with AD is the strongest, and we further substantiated this result by showing inverse correlations between VGF and β -amyloid and PHFtau tangles. Notably, prior studies on the VGF dysregulation in AD relied largely on case control comparison, and a direct association between human cortical VGF and molecular specific markers of AD has not been confirmed. The VGF association with neocortical Lewy bodies appears to be independent of AD, since the result persisted after adjusting for β -amyloid and tangles in the model. Interestingly, a study on VGF in CSF reported that the protein contributes to differentiating dementia with Lewy bodies from AD⁴². The association of VGF with LATE-NC has not been previously reported, but a lower VGF level was shown in ALS⁴³ and frontal temporal dementia⁴⁴, both of which also involve TDP43 pathology. In the current study, the association with LATE was attenuated by β -amyloid and PHFtau tangles, suggesting the result was likely confounded

by coexisting AD pathologies. No consistent signal was found for vascular conditions. Together, our investigation on neuropathologies reveals that VGF is primarily involved in Alzheimer's and Lewy bodies diseases.

We demonstrated that both VGF gene and protein are associated with late life cognitive health, and the associations of VGF are in part explained by neuropathologic indices. The implications of this finding are two fold. First, the association above and beyond neuropathologies would indicate that VGF is implicated in cognition via mechanisms that are not tied to common neuropathologies. Second, this finding helps to understand the role of VGF, as a potential target, along the neurodegenerative process. There is little consensus on whether VGF acts directly on reducing neuropathologies or downstream pathophysiological changes such as synapses loss due to neuropathologies. Data from animal models suggest that some VGF peptides regulate AD pathogenesis. An increase in germline *VGF* expression reduces the amyloid in transgenic mice brains, and injection of VGF-derived TLQP-62 peptide into the hippocampus of AD mice also reduced AD pathology¹². These results place VGF upstream of neuropathologies. An alternative theory proposed brain-derived neurotrophic factor (BDNF) as a target for synapse repair therapy⁴⁵. Unlike neuronal loss, damages to synapse are potentially reversible given their plasticity^{46, 47}, and neurotrophins promote synaptic transmission and growth. Based on this hypothesis, BDNF, possibly VGF as well, acts on synapse dysfunction that is caused by neuropathologies, which would place their role downstream of neuropathologies. Our data suggests that the associations of VGF gene expression and protein with cognitive decline are partially mediated by neuropathologies, not vice versa, which suggest that VGF is likely to exert at least part of its effect upstream of neuropathologies.

By leveraging snRNASeq data from over 400 human brains, we examined the cellular expressions of *VGF*. An earlier report based on data from Allen brain atlas¹⁴ showed that *VGF* is highly expressed in inhibitory GABAergic and excitatory glutamatergic neurons in the cortex, but the expression was not detected in other cell types. By contrast, our data suggest that while the gene is indeed highly expressed in neurons, it is also differentially expressed in other major cell types. Importantly, to our knowledge cell-type specific *VGF* expression with neuropathologies and cognitive decline has not been investigated before. Our analyses revealed that the associations are only detected in the excitatory and inhibitory neurons. These findings suggest that *VGF* gene expression may not be cell type specific, but its function is specific in neurons, or other cell types may not have proper regulatory mechanisms to tune the *VGF* expression. Of note, neurons are the most abundant nuclei in our data, and on average have more RNA than other cell types. As a result, estimates of *VGF* expression in glial cells are likely noisier, making it more difficult to detect an association.

For a protein target to be of therapeutic value, it is important to identify the actual biologically active form, peptide fragment in this case, and corresponding receptor that are functional. Of the dozen VGF-derived peptides annotated, TLQP-62 and TLQP-21 are the ones that have been extensively investigated, and each deliver protection against neuropathogenesis through distinct mechanisms¹⁴. Briefly, TLQP-62 promotes proliferation and reduces differentiation of neural progenitor cells by activating the BDNF/TrkB pathway, binding and activating ionotropic glutamate receptor. On the other hand, TLQP-21 binds

microglial receptors that regulates microglial phagocytosis and chemotaxis, which increases β -amyloid uptake and consequently reduces plaque formation and neuritic dystrophy. If these theories hold, TLQP-62 would likely be associated with cognitive outcome independent of AD pathologies, and by contrast, the association with TLQP-21 is likely through pathologies. We didn't have exact TLQP-62 or TLQP-21 peptide measured in SRM, but our data suggests that there is no specific VGF peptide fragment being exclusively associated with cognitive decline. More importantly, almost all the VGF peptide fragments show similar associations with neuropathologies. One explanation of these findings could be a lack of differential regulation across the VGF peptide fragments, thus they all correlate with each other given measured abundances.

VGF is proposed both as a potential biomarker and therapeutic target for AD as well as other degenerative disorders¹⁴. The data presented in this work could not distinguish the two. Instead, our findings revealed a complex role of VGF in brain health. First, VGF was involved in, not just one, but multiple degenerative conditions. This result indicates that VGF alone may not work as a specific disease biomarker. Second, VGF was associated with cognitive outcomes above and beyond neuropathologies known to cause dementia. This result indicates that VGF may represent a potential biomarker or therapeutic target for brain resilience against accumulating pathologies. Third, the lack of differential regulation across the VGF peptide fragments presents a challenge for target selection, and the therapeutic value of VGF warrants further investigation.

To our knowledge, this is by far the largest study that investigated human cortical VGF in relation to neuropathologies and late-life cognitive decline with high quality data. Multiple layers of gene expression and protein data were collected from the same brain region of DLPFC. Neuropathologic indices of AD, non-AD degeneration, and cerebrovascular diseases are systematically assessed blinded to clinical data, which allows for a comprehensive examination of VGF with all neuropathologies that most commonly exist in aging brain. Uniform cognitive evaluations are conducted annually and these densely spaced longitudinal data provide robust estimates of person specific cognitive change many years before death. In addition, the high follow-up (>90% among the survivors) and autopsy rates (>80%) of the ROSMAP cohorts reduce the bias due to attrition. Notably, the results across different layers of omics data are highly consistent, which adds robustness of our findings. Limitations are noted. ROSMAP are volunteer cohorts which require brain donation at death, and are not representative of general population. Participants are typically older, non-Latino whites and with high education. Separately, the analytic results from this work only provide supportive evidence for the role of VGF in neurodegenerative process, and do not infer causality.

Supplementary Material

Refer to Web version on PubMed Central for supplementary material.

Acknowledgement

The study was supported by National Institute on Aging grants R01AG17917, P30AG10161, P30AG072975, R01AG15819, R01AG067482, U01AG61356, and R01AG066831. This study would be not possible without the

contributions from all the ROSMAP participants, and we thank the investigators and staff at the Rush Alzheimer's Disease Center.

Data Availability

The datasets supporting the conclusions of this article can be requested for research purposes via Rush Alzheimer's Disease Center Research Resource Sharing Hub at <https://www.radc.rush.edu/>.

References

1. Selkoe DJ. Alzheimer's disease is a synaptic failure. *Science (New York, NY)*. 2002 Oct 25;298(5594):789–91.
2. Shankar GM, Li S, Mehta TH, et al. Amyloid-beta protein dimers isolated directly from Alzheimer's brains impair synaptic plasticity and memory. *Nature medicine*. 2008 Aug;14(8):837–42.
3. Milnerwood AJ, Raymond LA. Early synaptic pathophysiology in neurodegeneration: insights from Huntington's disease. *Trends in neurosciences*. 2010 Nov;33(11):513–23. [PubMed: 20850189]
4. Park H, Poo MM. Neurotrophin regulation of neural circuit development and function. *Nature reviews Neuroscience*. 2013 Jan;14(1):7–23. [PubMed: 23254191]
5. Ferri GL, Noli B, Brancia C, D'Amato F, Cocco C. VGF: an inducible gene product, precursor of a diverse array of neuro-endocrine peptides and tissue-specific disease biomarkers. *Journal of chemical neuroanatomy*. 2011 Dec;42(4):249–61. [PubMed: 21621608]
6. Lewis JE, Brameld JM, Jethwa PH. Neuroendocrine Role for VGF. *Frontiers in endocrinology*. 2015;6:3. [PubMed: 25699015]
7. Llano DA, Devanarayan P, Devanarayan V. VGF in Cerebrospinal Fluid Combined With Conventional Biomarkers Enhances Prediction of Conversion From MCI to AD. *Alzheimer disease and associated disorders*. 2019 Oct-Dec;33(4):307–14. [PubMed: 31305322]
8. Bai B, Wang X, Li Y, et al. Deep Multilayer Brain Proteomics Identifies Molecular Networks in Alzheimer's Disease Progression. *Neuron*. 2020 Mar 18;105(6):975–91 e7. [PubMed: 31926610]
9. Noda Y, Tanaka M, Nakamura S, et al. Identification of VGF nerve growth factor inducible-producing cells in human spinal cords and expression change in patients with amyotrophic lateral sclerosis. *International journal of medical sciences*. 2020;17(4):480–9. [PubMed: 32174778]
10. Henderson-Smith A, Corneveaux JJ, De Both M, et al. Next-generation profiling to identify the molecular etiology of Parkinson dementia. *Neurology Genetics*. 2016 Jun;2(3):e75. [PubMed: 27275011]
11. Khoonsari PE, Shevchenko G, Herman S, et al. Improved Differential Diagnosis of Alzheimer's Disease by Integrating ELISA and Mass Spectrometry-Based Cerebrospinal Fluid Biomarkers. *Journal of Alzheimer's disease : JAD*. 2019;67(2):639–51. [PubMed: 30614806]
12. Beckmann ND, Lin W-J, Wang M, et al. Multiscale causal networks identify VGF as a key regulator of Alzheimer's disease. *Nature communications*. 2020;11(1):1–19.
13. Wingo AP, Dammer EB, Breen MS, et al. Large-scale proteomic analysis of human brain identifies proteins associated with cognitive trajectory in advanced age. *Nature communications*. 2019;10(1):1–14.
14. Quinn JP, Kandigian SE, Trombetta BA, Arnold SE, Carlyle BC. VGF as a biomarker and therapeutic target in neurodegenerative and psychiatric diseases. *Brain communications*. 2021;3(4):fcab261. [PubMed: 34778762]
15. Schneider JA, Arvanitakis Z, Bang W, Bennett DA. Mixed brain pathologies account for most dementia cases in community-dwelling older persons. *Neurology*. 2007 Dec 11;69(24):2197–204. [PubMed: 17568013]
16. Rahimi J, Kovacs GG. Prevalence of mixed pathologies in the aging brain. *Alzheimer's research & therapy*. 2014;6(9):82.
17. Lin WJ, Jiang C, Sadahiro M, et al. VGF and Its C-Terminal Peptide TLQP-62 Regulate Memory Formation in Hippocampus via a BDNF-TrkB-Dependent Mechanism. *The Journal of*

- neuroscience : the official journal of the Society for Neuroscience. 2015 Jul 15;35(28):10343–56. [PubMed: 26180209]
18. Bozdagi O, Rich E, Tronel S, et al. The neurotrophin-inducible gene *Vgf* regulates hippocampal function and behavior through a brain-derived neurotrophic factor-dependent mechanism. *The Journal of neuroscience : the official journal of the Society for Neuroscience*. 2008 Sep 24;28(39):9857–69. [PubMed: 18815270]
 19. Alder J, Thakker-Varia S, Bangasser DA, et al. Brain-derived neurotrophic factor-induced gene expression reveals novel actions of VGF in hippocampal synaptic plasticity. *The Journal of neuroscience : the official journal of the Society for Neuroscience*. 2003 Nov 26;23(34):10800–8. [PubMed: 14645472]
 20. Cho K, Jang YJ, Lee SJ, et al. TLQP-21 mediated activation of microglial BV2 cells promotes clearance of extracellular fibril amyloid- β . *Biochemical and biophysical research communications*. 2020 Apr 9;524(3):764–71. [PubMed: 32037089]
 21. El Gaamouch F, Audrain M, Lin WJ, et al. VGF-derived peptide TLQP-21 modulates microglial function through C3aR1 signaling pathways and reduces neuropathology in 5xFAD mice. *Molecular neurodegeneration*. 2020 Jan 10;15(1):4. [PubMed: 31924226]
 22. Bennett DA, Buchman AS, Boyle PA, Barnes LL, Wilson RS, Schneider JA. Religious Orders Study and Rush Memory and Aging Project. *Journal of Alzheimer's disease : JAD*. 2018;64(s1):S161–S89. [PubMed: 29865057]
 23. Bennett DA, Schneider JA, Buchman AS, Mendes de Leon C, Bienias JL, Wilson RS. The Rush Memory and Aging Project: study design and baseline characteristics of the study cohort. *Neuroepidemiology*. 2005;25(4):163–75. [PubMed: 16103727]
 24. Bennett DA, Schneider JA, Arvanitakis Z, et al. Neuropathology of older persons without cognitive impairment from two community-based studies. *Neurology*. 2006 Jun 27;66(12):1837–44. [PubMed: 16801647]
 25. Boyle PA, Wilson RS, Yu L, et al. Much of late life cognitive decline is not due to common neurodegenerative pathologies. *Annals of neurology*. 2013 Sep;74(3):478–89. [PubMed: 23798485]
 26. Schneider JA, Arvanitakis Z, Yu L, Boyle PA, Leurgans SE, Bennett DA. Cognitive impairment, decline and fluctuations in older community-dwelling subjects with Lewy bodies. *Brain : a journal of neurology*. 2012 Oct;135(Pt 10):3005–14. [PubMed: 23065790]
 27. Nag S, Yu L, Capuano AW, et al. Hippocampal sclerosis and TDP-43 pathology in aging and Alzheimer disease. *Annals of neurology*. 2015 Jun;77(6):942–52. [PubMed: 25707479]
 28. Kapasi A, Yu L, Boyle PA, Barnes LL, Bennett DA, Schneider JA. Limbic-predominant age-related TDP-43 encephalopathy, ADNC pathology, and cognitive decline in aging. *Neurology*. 2020 Oct 6;95(14):e1951–e62. [PubMed: 32753441]
 29. Schneider JA, Wilson RS, Bienias JL, Evans DA, Bennett DA. Cerebral infarctions and the likelihood of dementia from Alzheimer disease pathology. *Neurology*. 2004 Apr 13;62(7):1148–55. [PubMed: 15079015]
 30. Boyle PA, Yu L, Nag S, et al. Cerebral amyloid angiopathy and cognitive outcomes in community-based older persons. *Neurology*. 2015 Dec 1;85(22):1930–6. [PubMed: 26537052]
 31. Arvanitakis Z, Capuano AW, Leurgans SE, Bennett DA, Schneider JA. Relation of cerebral vessel disease to Alzheimer's disease dementia and cognitive function in elderly people: a cross-sectional study. *The Lancet Neurology*. 2016 Aug;15(9):934–43. [PubMed: 27312738]
 32. Yu L, Tasaki S, Schneider JA, et al. Cortical Proteins Associated With Cognitive Resilience in Community-Dwelling Older Persons. *JAMA Psychiatry*. 2020 Nov 1;77(11):1172–80. [PubMed: 32609320]
 33. Tasaki S, Xu J, Avey DR, et al. Inferring protein expression changes from mRNA in Alzheimer's dementia using deep neural networks. *Nat Commun*. 2022 Feb 3;13(1):655. [PubMed: 35115553]
 34. Fujita M, Gao Z, Zeng L, et al. Cell-subtype specific effects of genetic variation in the aging and Alzheimer cortex. *bioRxiv*. 2022:2022.11.07.515446.
 35. Zheng GX, Terry JM, Belgrader P, et al. Massively parallel digital transcriptional profiling of single cells. *Nature communications*. 2017;8(1):1–12.

36. McGinnis CS, Murrow LM, Gartner ZJ. DoubletFinder: doublet detection in single-cell RNA sequencing data using artificial nearest neighbors. *Cell systems*. 2019;8(4):329–37. e4. [PubMed: 30954475]
37. Hao Y, Hao S, Andersen-Nissen E, et al. Integrated analysis of multimodal single-cell data. *Cell*. 2021;184(13):3573–87. e29. [PubMed: 34062119]
38. Law CW, Chen Y, Shi W, Smyth GK. voom: precision weights unlock linear model analysis tools for RNA-seq read counts. *Genome Biology*. 2014 2014/02/03;15(2):R29. [PubMed: 24485249]
39. Yu L, Petyuk VA, Gaiteri C, et al. Targeted brain proteomics uncover multiple pathways to Alzheimer's dementia. *Annals of neurology*. 2018 Jul;84(1):78–88. [PubMed: 29908079]
40. Hendrickson RC, Lee AY, Song Q, et al. High Resolution Discovery Proteomics Reveals Candidate Disease Progression Markers of Alzheimer's Disease in Human Cerebrospinal Fluid. *PLoS one*. 2015;10(8):e0135365. [PubMed: 26270474]
41. MacLean B, Tomazela DM, Shulman N, et al. Skyline: an open source document editor for creating and analyzing targeted proteomics experiments. *Bioinformatics*. 2010;26(7):966–8. [PubMed: 20147306]
42. van Steenoven I, Koel-Simmelink MJA, Vergouw LJM, et al. Identification of novel cerebrospinal fluid biomarker candidates for dementia with Lewy bodies: a proteomic approach. *Molecular neurodegeneration*. 2020 Jun 18;15(1):36. [PubMed: 32552841]
43. Brancia C, Noli B, Boido M, et al. TLQP Peptides in Amyotrophic Lateral Sclerosis: Possible Blood Biomarkers with a Neuroprotective Role. *Neuroscience*. 2018 Jun 1;380:152–63. [PubMed: 29588252]
44. van der Ende EL, Meeter LH, Stingl C, et al. Novel CSF biomarkers in genetic frontotemporal dementia identified by proteomics. *Annals of clinical and translational neurology*. 2019 Apr;6(4):698–707. [PubMed: 31019994]
45. Lu B, Nagappan G, Guan X, Nathan PJ, Wren P. BDNF-based synaptic repair as a disease-modifying strategy for neurodegenerative diseases. *Nature reviews Neuroscience*. 2013 Jun;14(6):401–16. [PubMed: 23674053]
46. Trachtenberg JT, Chen BE, Knott GW, et al. Long-term in vivo imaging of experience-dependent synaptic plasticity in adult cortex. *Nature*. 2002 Dec 19–26;420(6917):788–94. [PubMed: 12490942]
47. Holtmaat A, Svoboda K. Experience-dependent structural synaptic plasticity in the mammalian brain. *Nature reviews Neuroscience*. 2009 Sep;10(9):647–58. [PubMed: 19693029]

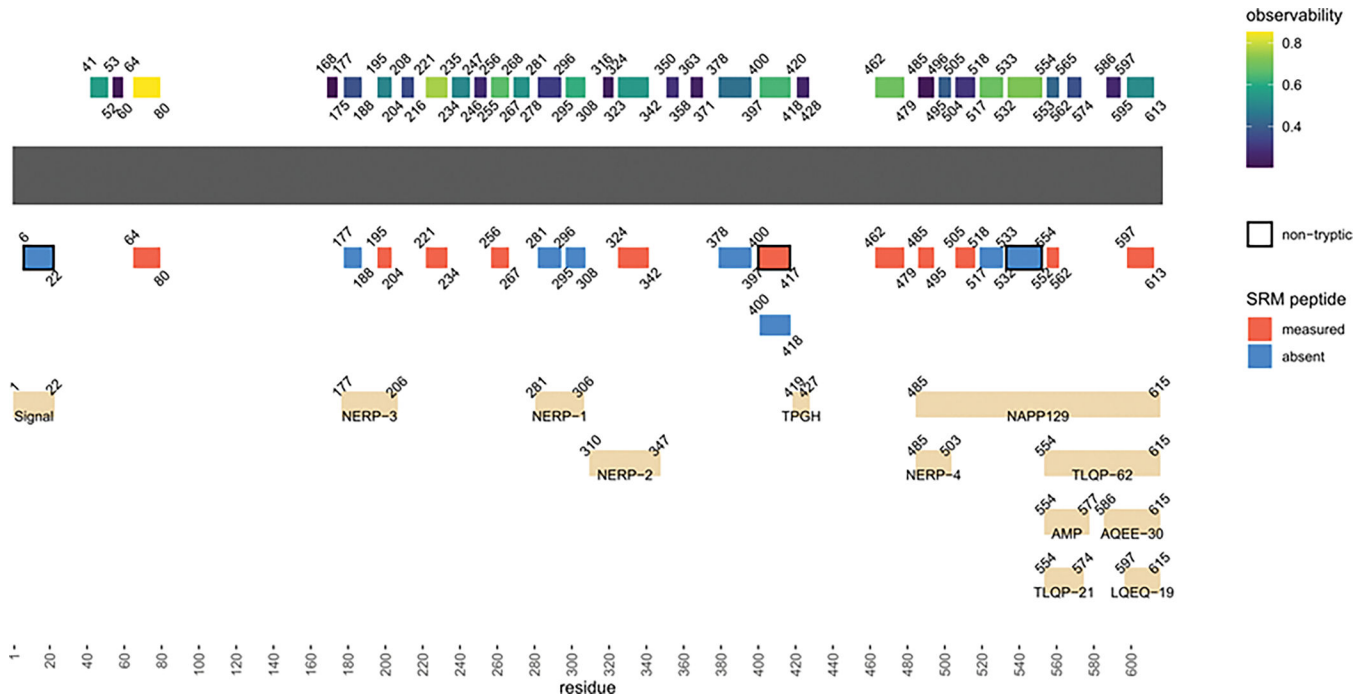


Figure 1. illustrates the schematic of human VGF polypeptide. The dark gray band represents the whole length of the VGF original protein. Above we show peptides resulting from *in silico* trypsin digest. To ensure compatibility with SRM assay, we retained only the ones longer than 6 and shorter than 22 amino acids. The predicted LC-MS observability score is coded using viridis color scheme. Right below the VGF protein we show tryptic peptides selected for SRM assay. Red and blue colors denote if the signal coming from endogenous tryptic or partially peptide was sufficient to measure or below the detection limit, respectively. The peptides that required non-tryptic cleavage labeled with black boxes. The annotation of the VGF with known biologically active fragments, based on prior literature, is shown at the bottom.

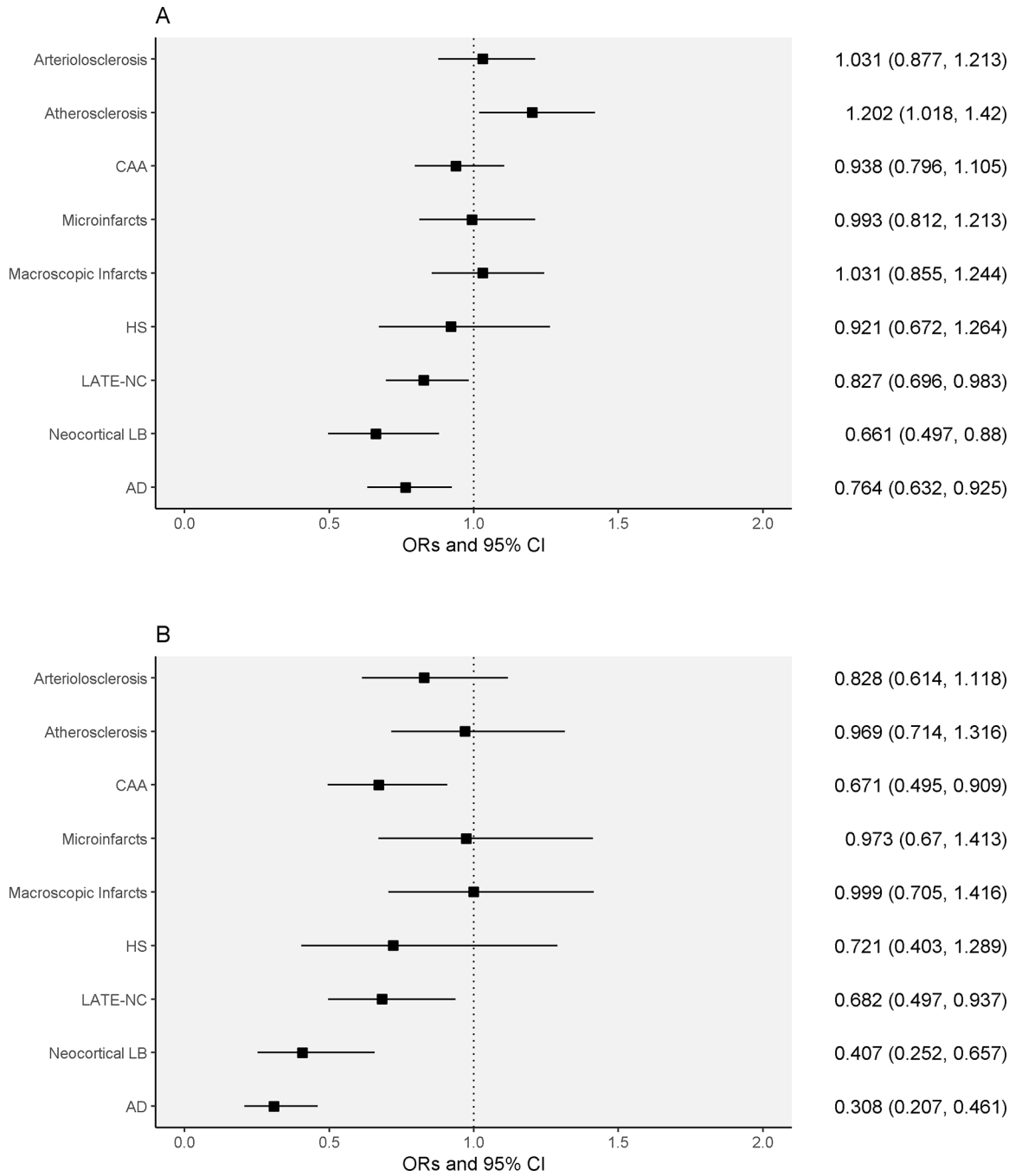


Figure 2. illustrates the associations of the bulk *VGF* gene expression (A), and separately the *VGF* protein (B), with common neuropathologies. For each neuropathologic index, the black square and horizontal line segment represent the odds ratio and corresponding 95% confidence interval. To reduce false positives due to multiple testing, the 95% confidence intervals were computed using $\alpha_{adj}=0.005$. Line segment that did not cross the vertical dotted line of 1 suggests a significant association of *VGF* with the corresponding neuropathology.

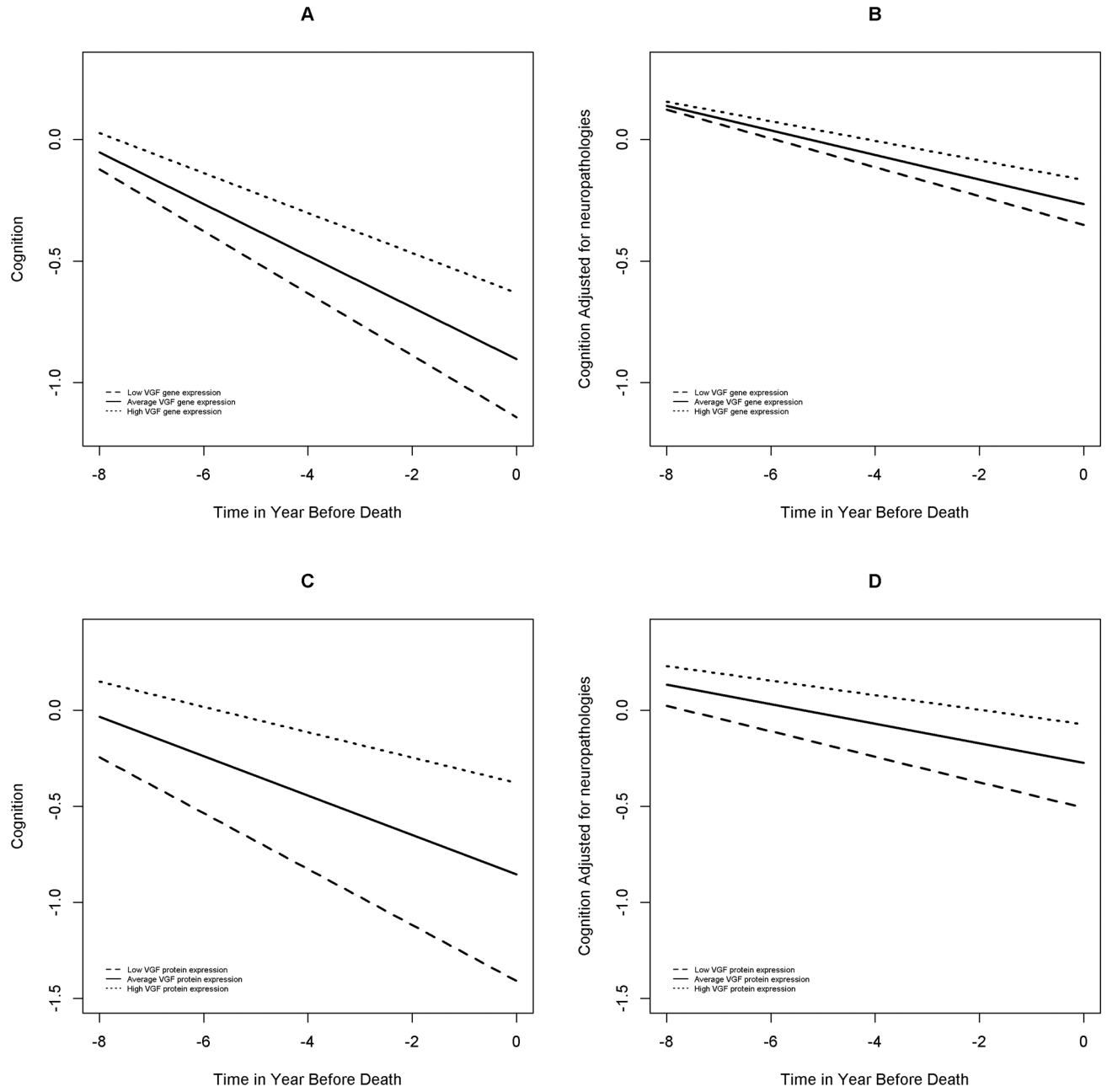


Figure 3. illustrates the associations of the bulk *VGF* gene expression (A and B), and separately the *VGF* protein (C and D), with late life cognitive decline before and after adjusting for neuropathologies.

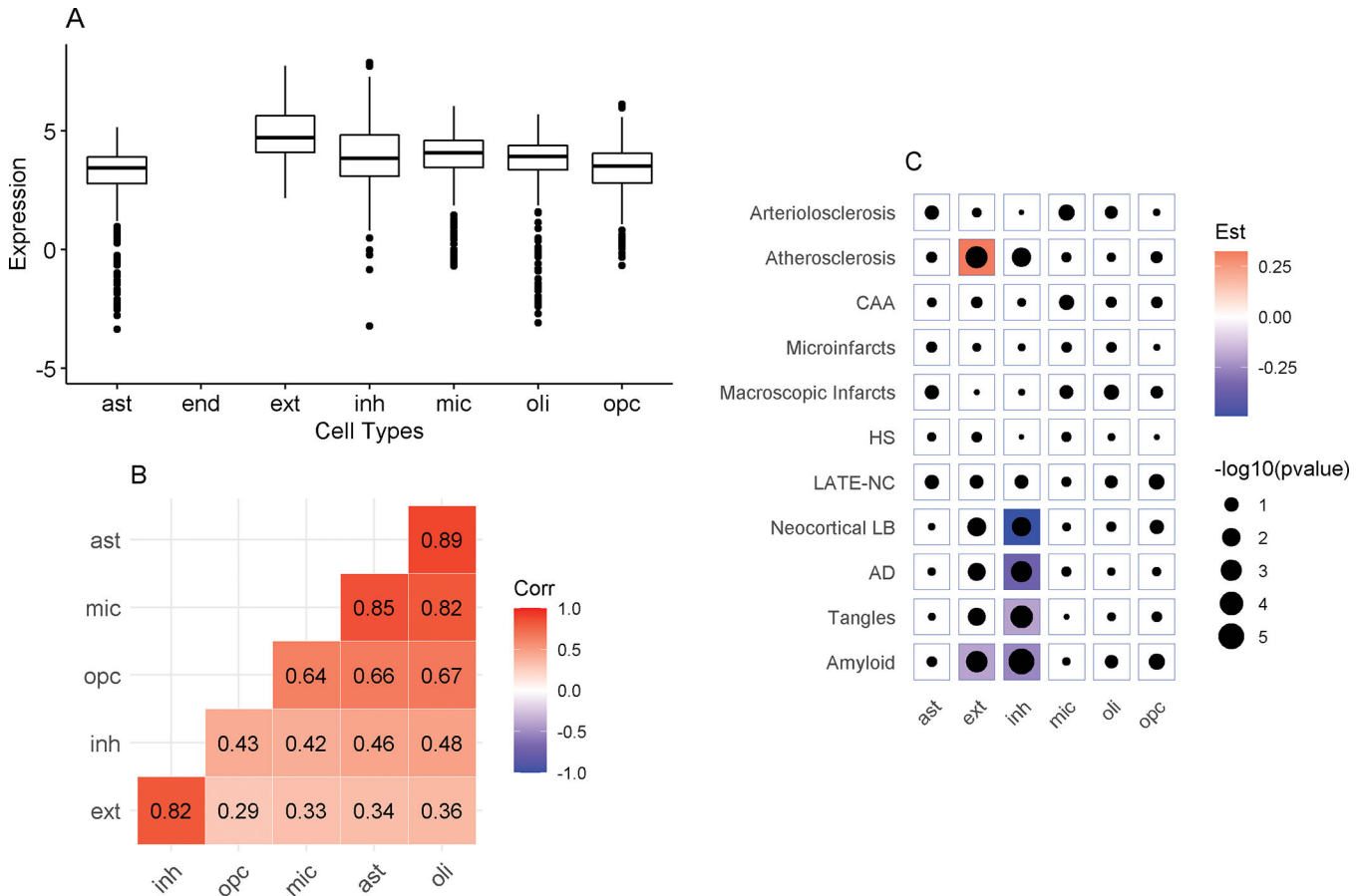


Figure 4. illustrates the cellular *VGF* expressions and the associations with neuropathologies. The *VGF* gene expression levels across the 7 major cell types are presented as a box plot (A). The pairwise correlations between these cellular expressions are shown as a triangle matrix (B), with cell-types rearranged to highlight the correlated clusters. The associations with neuropathologies are shown as a heatmap (C). The cell types are on the x-axis, and neuropathologies are on the y-axis. Red tile represents a significant positive association (i.e. higher expression is associated with more or higher odds of the pathology) and blue tile represents a significant negative association (i.e. higher expression is associated with less or lower odds of the pathology). Statistical significance was determined using $\alpha_{adj}=0.005$. The size of black dot inside the tile signifies the strength of an association. Cell types: ast: astrocytes, end: endothelial cells, ext: excitatory neurons, inh: inhibitory neurons, mic: microglia, oli: oligodendrocytes, and opc: oligodendrocyte precursor cells.

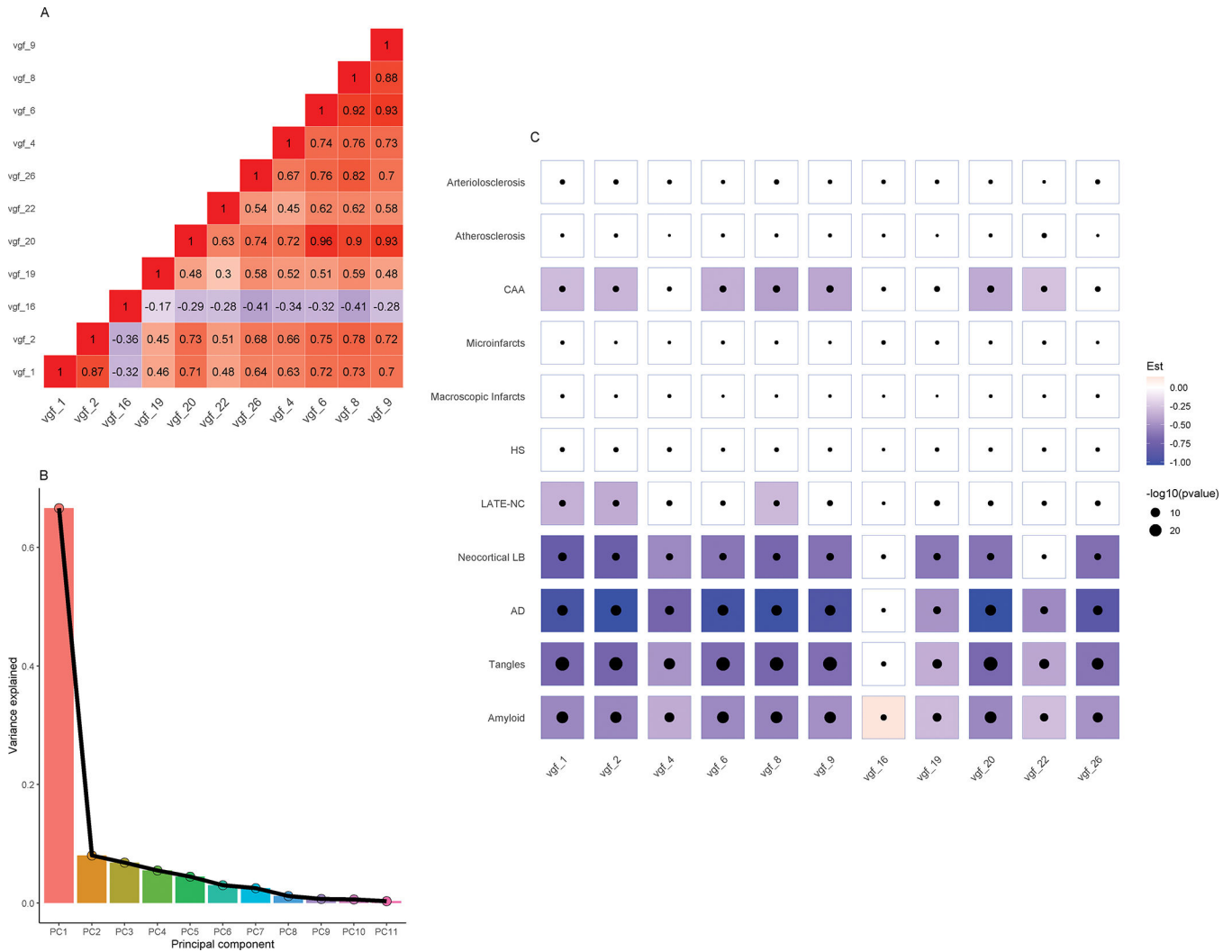


Figure 5. illustrates the VGF peptide fragments and the associations with neuropathologies. The pairwise correlations of the abundance between the VGF peptide fragments are shown as a triangle matrix (A). The result from a principal component analysis was summarized as a scree plot which describes the decomposition of total variance by each principal component (B). The associations with neuropathologies are shown as a heatmap (C). The peptide fragments are on the x-axis, and neuropathologies are on the y-axis. Red tile represents a significant positive association (i.e. higher abundance is associated with more or higher odds of the pathology) and blue tile represents a significant negative association (i.e. higher abundance is associated with less or lower odds of the corresponding pathology). Statistical significance was determined using $\alpha_{adj}=0.005$. The size of black dot inside the tile signifies the strength of an association.

Table 1

Demographic, clinical and neuropathologic characteristics

	Bulk Sample (N=1020)	Single Nuclei Sample (N=424)
Age at baseline, years [†]	80.8 (6.9)	81.3 (7.1)
Age at death, years [†]	89.5 (6.5)	89.2 (6.8)
Female	694 (68.0%)	288 (67.9%)
Education, years [†]	16.2 (3.6)	16.3 (3.5)
<i>APOE</i> ε4 carriers	258 (25.5%)	109 (25.8%)
Clinical diagnosis		
No cognitive impairment	333 (32.7%)	143 (33.7%)
Mild cognitive impairment	249 (24.4%)	110 (25.9%)
Dementia	438 (42.9%)	171 (40.3%)
Alzheimer's disease	649 (63.6%)	266 (62.7%)
Aβ load [§]	3.54 (0.64–7.27)	3.01 (0.51–7.41)
PHFtau tangle density [§]	4.04 (1.62–8.26)	3.82 (1.49–7.80)
Neocortical Lewy bodies	131 (12.9%)	33 (7.8%)
Hippocampal sclerosis	94 (9.3%)	38 (9.0%)
LATE-NC		
Stage 0	479 (48.3%)	189 (47.1%)
Stage 1	198 (20.0%)	88 (22.0%)
Stage 2	97 (9.8%)	45 (11.2%)
Stage 3	217 (21.9%)	79 (19.7%)
Chronic macroscopic infarcts	368 (36.1%)	159 (37.5%)
Chronic microinfarcts	284 (27.8%)	109 (25.7%)
Cerebral amyloid angiopathy		
None	228 (22.7%)	98 (23.5%)
Mild	427 (42.5%)	178 (42.7%)
Moderate	223 (22.2%)	94 (22.5%)
Severe	127 (12.6%)	47 (11.3%)
Atherosclerosis		
None	192 (18.9%)	52 (12.3%)

	Bulk Sample (N=1020)	Single Nuclei Sample (N=424)
Mild	480 (47.1%)	197 (46.7%)
Moderate	270 (26.5%)	125 (29.6%)
Severe	76 (7.5%)	48 (11.4%)
<hr/>		
Arteriolosclerosis		
None	295 (29.1%)	116 (27.6%)
Mild	376 (37.1%)	144 (34.2%)
Moderate	263 (25.9%)	114 (27.1%)
Severe	80 (7.9%)	47 (11.2%)

[†] Mean (Standard deviation)

N(%)

[§] Median (Interquartile range); MMSE: Mini-mental state examination; LATE-NC: Limbic predominant age-related TDP-43 encephalopathy neuropathologic changes.

Table 2

VGF peptides with cognitive decline

Fragments	Estimate	Standard error	95% CI	<i>p</i>
VGF #1	0.053	0.005	0.038, 0.068	<.001
VGF #2	0.057	0.006	0.041, 0.073	<.001
VGF #4	0.032	0.005	0.018, 0.046	<.001
VGF #6	0.048	0.005	0.033, 0.063	<.001
VGF #8	0.052	0.006	0.037, 0.068	<.001
VGF #9	0.045	0.005	0.030, 0.059	<.001
VGF #16	-0.002	0.004	-0.013, 0.010	0.720
VGF #19	0.028	0.005	0.015, 0.041	<.001
VGF #20	0.049	0.005	0.033, 0.064	<.001
VGF #22	0.027	0.005	0.013, 0.040	<.001
VGF #26	0.043	0.006	0.026, 0.060	<.001

Each row was extracted from a separate linear mixed model with annual cognitive scores as the longitudinal outcome and the abundance of individual VGF peptide the predictor. The models were adjusted for age, sex and education. The estimate corresponds to the interaction term between VGF peptide and time in years before death, which capture the peptide association with the slope of cognitive change. 95% CI: the 95% confidence intervals were calculated using $\alpha_{adj}=0.005$.